Polymer 51 (2010) 5490–5499

Contents lists available at ScienceDirect

Polymer

journal homepage: www.elsevier.com/locate/polymer

Comparative studies on effects of silica and titania nanoparticles on crystallization and complex segmental dynamics in poly(dimethylsiloxane)

P. Klonos [a,*], A. Panagopoulou [a], L. Bokobza [b], A. Kyritsis [a], V. Peoglos [a], P. Pissis [a]

[a] Department of Physics, National Technical University of Athens, Zografou Campus, 15780, Athens, Greece
[b] Laboratoire PPMD, E.S.P.C.I., 10 rue Vauquelin, 75231 Paris Cedex, France

ARTICLE INFO

Article history:
Received 18 August 2010
Received in revised form
20 September 2010
Accepted 20 September 2010
Available online 26 September 2010

Keywords:
Poly(dimethylsiloxane) nanocomposites
Segmental dynamics
Polymer crystallization

ABSTRACT

Effects of *in situ* synthesized silica and titania nanoparticles, 5 and 20–40 nm in diameter, respectively, on glass transition and segmental dynamics of poly(dimethylsiloxane) networks were studied by employing differential scanning calorimetry, thermally stimulated depolarization currents and broadband dielectric relaxation spectroscopy techniques. Strong interactions between the well dispersed fillers and the polymer suppress crystallinity and affect significantly the evolution of the glass transition in the nanocomposites. Next to the α relaxation associated with the glass transition of the bulk amorphous polymer fraction, two more segmental relaxations were recorded, originating from polymer chains restricted between condensed crystal regions (α_c-relaxation) and the semi-bound polymer in an interfacial layer with strongly reduced mobility due to interactions with hydroxyls on the nanoparticle surface (α' relaxation), respectively. Interactions with the polymer were found to be stronger in the case of titania than silica, leading to an estimated interaction length of around 2 nm for silica and at least double for titania nanocomposites.

1. Introduction

The evolving needs for multifunctional materials aiming at complex applications, is a basic motivation for modern science to improve or, as a second step, to create good material properties. As a new option, the development of various composite polymeric materials [1] was a satisfactory solution for various needs and applications. For the last years, nanoscale composites are in the center of interest [2]. The use of nanoscale fillers in a composite material offers the great benefit that, in comparison with traditional composites, only a small amount of filler content is sufficient to induce tremendous improvements in desired properties [3]. The main reason for that is the surface to volume ratio of the nanoparticles, which is very high in the nanocomposites, in comparison with traditional composites. Specifically, the polymer fraction close to these surfaces (interfacial polymer) constitutes a significant fraction of the material and its behaviour affects significantly or even dominates the properties of the system. It is commonly accepted that the improvement of properties in polymer nanocomposites is related to modified polymer dynamics in the interfacial layer [4,5].

The presence of various nanofillers, such as silica, titania, nanoclays, typically leads to a restriction of polymer mobility and thermal transitions ability, manifested in an increase of the glass transition temperature, and a decrease of the degree of crystallinity and of the crystallization temperature in semi-crystalline polymer matrices [6–8]. The extent of these effects depends on composition and preparation/processing conditions and can be further controlled by functionalization of either the polymer or the filler [9,10]. There are, however, several exceptions to this behaviour, depending on the type of polymer and filler [11] and/or the preparation/processing conditions [12]. It is referred that carbon nanotubes in polymer/carbon nanotube nanocomposites [13] and clays in polymer nanocomposites [9,14] act as crystallization nuclei or favor different types of crystals growth.

Similar to the picture described above for polymer nanocomposites, results in literature on effects of nanoparticles on glass transition and segmental dynamics in rubber/oxide nanocomposites, in particular rubber/silica nanocomposites, appear, at least at first glance, controversial [8,15–20]. Depending on composition, the method of preparation and the experimental technique employed, results on glass transition and segmental dynamics have often been described in term of a three layer model [15–17] or a two layer model [18–20] or a continuous distribution of glass transition temperatures as a function of the distance from the particle surface [21]. Rittigstein and Torkelson pointed to the significance of the type of polymer–filler interaction and, for a given composition, of the method of preparation [12]. Roland and

* Corresponding author. Tel.: +30 210 772 2974; fax: +30 210 772 2932.
E-mail address: pklonos@central.ntua.gr (P. Klonos).

0032-3861/$ – see front matter © 2010 Elsevier Ltd. All rights reserved.
doi:10.1016/j.polymer.2010.09.054

coworkers pointed out that different experimental techniques may result to different pictures of dynamics in the nanocomposites, which are not necessarily contradictory [22].

In the present work we study polymer–filler interactions and their effects on molecular mobility in PDMS networks filled *in situ* with silicon and titanium oxide nanoparticles generated via sol–gel technique. To that aim, we employ differential scanning calorimetry (DSC), and two dielectric techniques, thermally stimulated depolarization currents (TSDC) and dielectric relaxation spectroscopy (DRS), covering together a broad frequency range of 10^{-4} to 10^{6} Hz. Morphological characterization of the materials in a previous paper showed a good dispersion of nanoparticles, 5 and 20–40 nm in diameter for silica and titania nanocomposites, respectively, and revealed fine details of this dispersion [23]. The mechanical properties were significantly improved in a different way for the two oxides, and that was correlated with the different strength of polymer–filler interaction and details of the nanoparticle dispersion [23]. The results of the present study show significant effects of the nanoparticles on segmental dynamics associated with the glass transition, originating from the severe restriction of crystallization ability and the strong reduction of molecular mobility in an interfacial layer of a few nm in thickness around the nanoparticles. The extent of these effects depends on the type of the filler (stronger for titania than for silica) and the quality of particle dispersion. The effects are quantified and the results may provide a basis for understanding and modeling the improvement of mechanical properties at the molecular level.

From the methodological point of view, the results of the present study illustrate the power of the two dielectric techniques used in combination with DSC for the investigation of effects of nanofiller on thermal transitions and molecular dynamics in the nanocomposites under investigation [8]. In that respect, the dielectric techniques, implemented also in several other fields of macromolecular science [24,25], compete with and complement other methods employed, such as dynamic mechanical analysis measurements [8,15], changes in viscoelasticity [22] and DSC glass transition step [8,26,27], electron spin resonance [28] and fluorescence/multilayer methods [12].

2. Experimental

2.1. Materials

PDMS networks filled with several contents of silica (~6–36 wt %) and titania (~5–18 wt%) amorphous nanoparticles and, for comparison, unfilled PDMS networks were studied in the present work. The unfilled polymer network was prepared from hydroxyl-terminated PDMS (Gelest, $M_w = 18000$) by end-linking reactions using tetraethoxysilane (TEOS) as cross-linking agent. For composites preparation the unfilled extracted polymer network was swollen in TEOS for silica or in titanium (IV) n-butoxide (TBO) for titania, which were the precursors of the particles generation in the sol–gel process. Then the samples were hydrolyzed during 48 h and vacuum-dried at 80 °C for several days to constant weight. The amount of filler is represented by the difference between the final and initial weights. Films of ~1 mm in thickness were the finally produced samples [23].

According to the statistical equation $\langle r^2 \rangle = C_\infty / nl^2$ [29], by knowing the average number and length of the main-chain bond length, n and l respectively, the characteristic ratio C_∞ and considering that crosslinking involves only the endgroups of the PDMS chains, the end-to-end distance between crosslinks $\langle r^2 \rangle^{1/2}$ was calculated around 11.2 nm. Transmission electron microscopy (TEM), small-angle neutron scattering (SANS), stress–strain and equilibrium swelling measurements were carried out on the same systems [23]. Results showed that silica nanoparticles are well dispersed in the polymer matrix with small domains around ~5 nm in diameter and rather diffuse surfaces. At higher than 10 wt% contents an interpenetrated polymer–silica structure is obtained. On the other hand, titania particles seem to be approximately spherical in shape with diameters between 20 and 40 nm and better defined interfaces with PDMS than in the case of silica. Even at the lowest titania content the particles are almost connected in a branched network structure. Distribution is better in case of silica giving a higher polymer–filler interfacial area but weaker bonds with PDMS, comparing with the strong PDMS–titania interactions. Mechanical measurements showed higher reinforcement of PDMS in case of silica. Tense transitions from linear (elastic) to sigmoidal (plastic) stress–strain behaviour for ~18 wt% SiO_2 and ~8 wt% TiO_2 were observed, due to the forming of the inorganic networks at these compositions [23]. The interactions of PDMS chain segments with the nanoparticles occur via hydroxyl groups (–OH) on the surfaces of the nanoparticles, which are proved by solid-state ^{29}Si NMR, Infrared (IR) and near-IR spectroscopy, as shown in previous work for PDMS/silica nanocomposites [30].

It is useful to note that the measurements described above were performed at room temperature, where this polymer, semi-crystalline at lower temperatures, is fully amorphous. So any effects in mechanical and swelling properties are affiliated only to filler–polymer and filler–filler interactions [23].

2.2. Differential scanning calorimetry

Thermal properties of the materials were investigated in helium atmosphere in the temperature range from –170 to 40 °C using a TA Q200 series DSC instrument. Samples of ~8 mg in mass, cut from the produced films, were closed in standard Tzero aluminium pans. Cooling and heating rates were fixed to 10 °C/min for typical measurements. In order to enhance cold crystallization event, affiliated to the suppression of crystallization (during cooling) due to the presence of nanoparticles, measurements were carried out also using different cooling rates (5, 10 and 20 °C/min) and fixed heating rate (at 10 °C/min). At this point it is useful to note that PDMS crystals are melted at room temperature, so a first heating scan for erasing thermal history [31] was not necessary here.

2.3. Thermally stimulated depolarization currents

Thermally stimulated depolarization currents (TSDC) is a special dielectric technique in the temperature domain, characterized by high sensitivity and high resolving power, the latter arising from its low equivalent frequency (10^{-4} to 10^{-2} Hz) [32]. By this technique, the sample (15–20 mm in diameter and ~1 mm in thickness) was inserted between the brass plates of a capacitor, placed in a Novocontrol TSDC sample cell and polarized by an electrostatic field E_p (~100 V/mm) with a home-made voltage source at polarization temperature $T_p = 20$ °C for time $t_p = 5$ min. With the field still applied, the sample was cooled down to –150 °C (cooling rate 10 °C/min, under nitrogen flow), sufficiently low to prevent depolarization by thermal energy, then short-circuited and reheated up to 50 °C at a constant heating rate $b = 3$ °C/min. Temperature control was achieved by means of a Novocontrol Quatro cryosystem. A discharge current was generated during heating and measured as a function of temperature with a sensitive programmable Keithley 617 electrometer.

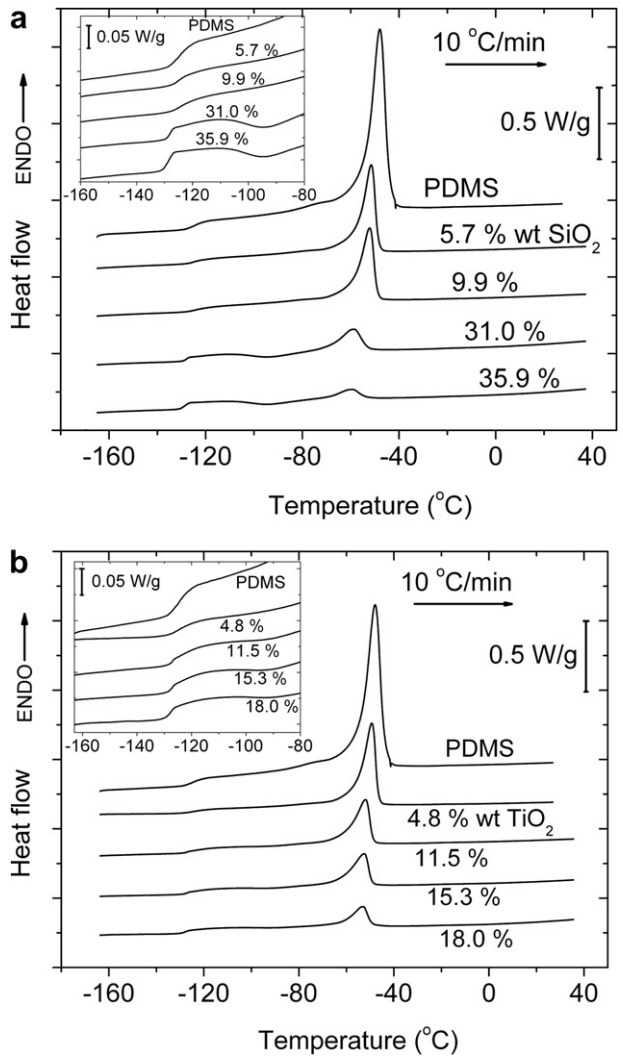

Fig. 1. Comparative DSC thermograms for unfilled PDMS, (a) PDMS/silica and (b) PDMS/titania nanocomposites during heating. Glass transition steps and melting peaks are observed for all samples. The insets show details in the glass transition region.

2.4. Dielectric relaxation spectroscopy

For dielectric relaxation spectroscopy (DRS) measurements [33] the sample (same as that used for TSDC measurements) was placed between the plates of a capacitor and an alternate voltage was applied in a Novocontrol sample cell. The complex dielectric permittivity, $\varepsilon^* = \varepsilon' - i\varepsilon''$, was recorded isothermally as a function of frequency in the range 10^{-1} to 10^6 Hz at temperatures −150 to 20 °C (in nitrogen atmosphere) in steps of 2.5, 5 and 10 °C (depending on the process to be studied) using a Novocontrol Alpha analyzer. The temperature was controlled to better than 0.5 °C with a Novocontrol Quatro cryosystem. This measurement protocol will be referred to as *protocol A*. In order to investigate effects of crystallinity on the segmental dynamics, measurements were carried out also after a 30 min isothermal stay (annealing) of the sample at a temperature between the onset and the peak of crystallization event, as it was defined from DSC measurements, this annealing leading to maximum degree of crystallinity. This measurement protocol will be referred to as *protocol C*. Finally, DRS measurements were also carried out isothermally at a temperature close to crystallization temperature. Continuous frequency scans taken every 15 min provided an almost online view of changes in the dielectric response related to segmental dynamics in the course of evolution of the crystallization process [34,35].

3. Results and discussion

3.1. DSC measurements

DSC measurements for PDMS/silica and PDMS/titania nanocomposites and for comparison unfilled PDMS are presented in Fig. 1. Heating scans are shown in these thermograms, comparing the changes in the thermal transitions of the polymer in the temperature range from −170 to 40 °C with the successive increasing of filler content. All the respective recorded and calculated values of interest are shown in Table 1.

The heating scans in Fig. 1a and b, for PDMS/silica and PDMS/titania, respectively, followed the cooling scans (not shown here) in the same temperature range and rate (10 °C/min). In these cooling scans a single exothermic peak was observed around −103 to −78 °C, representing the crystallization event [1,36], and an endothermic step in the baseline around −130 to −125 °C, representing the glass transition of PDMS. In previous studies on linear and crosslinked PDMS systems [8,36–39] the glass transition temperature has been observed between −130 and −115 °C and the crystallization temperature between −100 and −76 °C.

During heating the glass transition is recorded for all samples and the characteristic temperature T_g, determined as the midpoint of the heat capacity step at glass transition, obtained between −129 and −123 °C. As temperature increases, in the case of nanocomposites with high filler contents, 31 wt% silica and higher and 18 wt% titania and higher, an exothermic event is observed close to T_c region, representing cold crystallization [31]. This is a result of uncompleted crystallization during cooling. For lower filler contents and pure PDMS this phenomenon is absent, indicating that at this cooling rate (10 °C/min) crystallization is completed.

Table 1.
Crystallization, melting and glass transition temperatures T_c, T_m and T_g respectively, normalized respective enthalpies $\Delta H_{c/m,norm}$ and degree of crystallinity X_c, normalized heat capacity step of glass transition $\Delta C_{p,norm}$, calculated amount and estimated thickness of immobilized polymer layer on the nanoparticles X_{imm} and d_{imm} respectively, for PDMS, PDMS/silica and PDMS/titania nanocomposites.

Sample	X_{filler} (wt%)	X_{filler} (vol%)	T_c (°C)	$\Delta H_{c,norm}$ (J/g_{PDMS}) (±1)	X_c (±5%)	T_m (°C)	$\Delta H_{m,norm}$ (J/g_{PDMS}) (±1)	T_g (°C) (±0.5)	$\Delta C_{p,norm}$ (J/g °C) (±0.01)	X_{imm} (±10%)	d_{imm} (nm) (±25%)
PDMS	0	0	−78	30	0.80	−48	31	−124	0.81	–	–
+TiO_2	4.8	1.9	−78	16	0.43	−49	15	−124	0.16	0.80	38
	11.5	4.7	−81	11	0.29	−52	11	−125	0.18	0.78	24
	15.3	6.4	−82	9	0.23	−52	9	−126	0.20	0.75	20
	18.0	7.7	−85	5	0.13	−53	5	−127	0.17	0.79	19
+SiO_2	5.7	3.3	−81	16	0.42	−52	16	−124	0.16	0.80	5
	9.9	6.0	−82	15	0.39	−52	14	−123	0.17	0.78	4
	31.0	22.3	−97	5	0.14	−59	8	−128	0.14	0.83	2
	35.9	26.0	−103	1	0.04	−60	4	−129	0.22	0.73	1

Combining our observations on the crystallization-melting changes of PDMS, we gain strong indications that the addition of the fillers restricts the creation of crystallization nuclei [36], so crystallization in these materials takes place not close to the nanoparticles.

In general and just by comparing pure semi-crystalline polymeric materials at standard measurement procedures, cold crystallization is stronger in linear polymers than in networks [36], which means that the networks get easier crystallized [29]. Any factor that suppresses crystallinity (e.g. the absence of crosslinking or addition of filler, non-interacting with the polymer) can give rise to cold crystallization. An interesting result with respect to cold crystallization is presented in Fig. 2 for PDMS + 11.5 wt% titania at different cooling rates. By cooling the sample at 5 °C/min, more time is given for crystallization to be completed, than by cooling at the higher rates of 10 and 20 °C/min. So cold crystallization is observed, during standard heating at 10 °C/min, only for the samples that were previously crystallized at high cooling rates. Please note that the heat flow values in Fig. 2 are normalized with the respective temperature rates. Although crystallization area (ΔH_c) and T_m are depressed at higher cooling rates, no significant changes are observed on the glass transition.

Coming back to Fig. 1, at higher temperatures, complex endothermic melting peaks are observed between −60 and −48 °C. Complex and double melting peaks have been observed before in PDMS systems [36–38]. The secondary weaker melting peak precedes the main one by 15–20 °C. Two possible explanations about its origins [36] are as follows: (a) during heating small metastable crystals [40] melt, then get recrystallized and melt again into the main event or (b) the two melting peaks correspond to different types of crystallites. DSC measurements of crystallization annealing *protocol C* (not shown here) provide support for explanation (a). For the materials of the present work the origins and effects on the molecular mobility, in general, of these complex peaks are still under investigation and will be discussed in future work.

Using the respective enthalpies $\Delta H_{c/m,norm}$ as recorded through DSC and also normalized to the same polymer content X_{PDMS} for each sample (Eq. (1)), the degree of crystallinity X_c was calculated according to Eq. (2), in which $\Delta H_{100\%}$ is the enthalpy of PDMS fusion, taken as 37.43 J/g [36].

$$\Delta H_{c,norm} = \Delta H_{c,DSC}/X_{PDMS} \quad (1)$$

$$X_c = \Delta H_{m,norm}/\Delta H_{100\%} \quad (2)$$

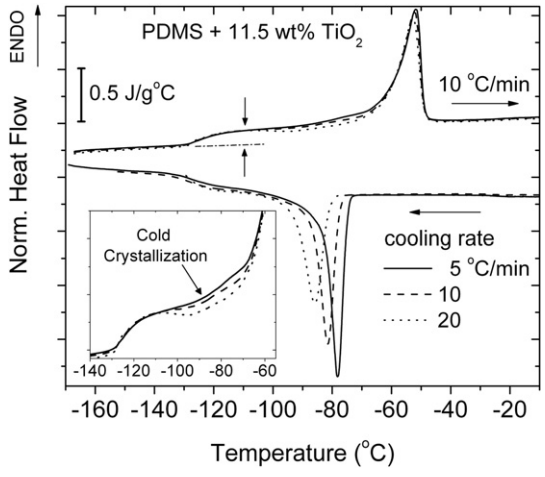

Fig. 2. DSC thermograms for PDMS + 11.5 wt% titania nanocomposite for cooling rates 5, 10 and 20 °C/min. After fast cooling cold crystallization is observed during heating. The inset shows in more detail the temperature region of glass transition and crystallization.

The results (Table 1, Figs. 3 and 4) show that the crystallization temperature and the degree of crystallinity systematically decrease with the increasing of filler content. In particular, we see in Fig. 3 that the depression of T_c with the addition of silica is significant even at the lowest content, from −78 for neat PDMS to −103 °C for the highest loading, almost linearly. On the other hand, in the case of titania significant changes on T_c start at about 10 wt% of filler content, but then follow a similar (parallel) trend as in silica. In Fig. 4 one can observe that by adding about 5 wt% of nanoparticles, silica or titania, the crystallinity degree of PDMS drops from 0.80 to 0.43. For further filler addition it is clear that the suppression of X_c is by far stronger in the case of titania. Thus, by comparing with each other the two types of nanocomposites in Figs. 3 and 4, we conclude that titania is more effective than silica in suppressing X_c and less effective in reducing T_c. Taking a glance on the melting temperature values (Table 1) one can observe that the addition of filler depresses also T_m, e.g. by 12 °C at the maximum loading. The reduction of the values is again similar for PDMS/silica and PDMS/titania composites, indicating similar size and quality of crystals.

These results suggest that the interactions between the particles and PDMS (hydrogen bonding between the oxygens on the polymer backbone and the hydroxyls on the nanoparticle surfaces) strongly suppress the creation of crystallization nuclei and the growth and quality of the PDMS spherulites [40] in the nanocomposites. The depression of crystallization and melting enthalpies have very similar trends and show that the changes become stronger as the filler content gets higher than about 10 wt% for silica and about 8 wt % for titania, as compared to lower contents. Such behaviour could be explained in terms of the formation of an inorganic network throughout the polymer volume at these and higher filler contents, respectively, for the two types of filler. Such an inorganic network could be the main reason for the restriction of growing of crystals, due to the reduction of regions of free polymer mobility. The above results and suggestions for their explanation come in agreement with the results of TEM and stress–strain measurements on the same compositions [23]. Formation of an inorganic silica network was observed also in poly(hydroxyethyl acrylate)/silica nanocomposites, where, similar to here, silica particles were generated by sol–gel process [6].

In the insets to Fig. 1 we can observe changes in the glass transition step with composition. For both cases of filler, T_g decreases by 1–4 °C with the addition of filler, this decrease being stronger in the case of titania for comparable filler fractions (Table 1). A possible explanation for this behaviour is the reduction of the degree of

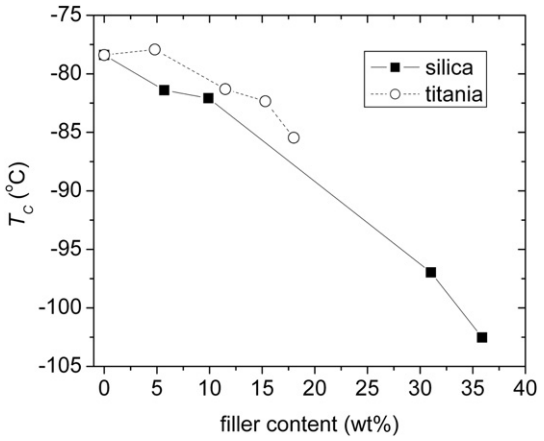

Fig. 3. Depression of PDMS crystallization temperature with the addition of silica and titania nanoparticles.

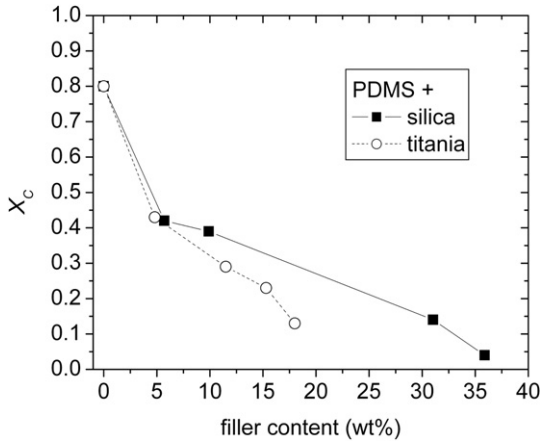

Fig. 4. Degree of crystallinity for PDMS and different compositions of PDMS/silica and PDMS/titania nanocomposites.

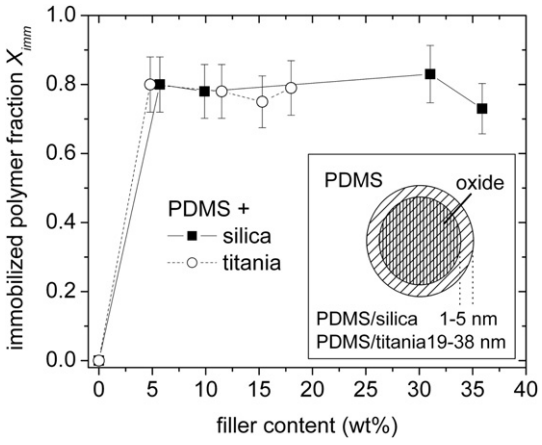

Fig. 5. Fraction of the amorphous polymer immobilized on the surfaces of the nanoparticles for PDMS/silica and PDMS/titania nanocomposites, as calculated from Eq. (4). The inset shows the simplified model used to calculate the thickness of the interfacial layer.

crystallinity with increasing filler content of the nanocomposites [29]. Another quantity of interest in Fig. 1 is the width of the glass transition, the difference between the onset and the completion temperature, $T_{end} - T_{onset}$, which is ~5 °C for PDMS, gets broadened to 8–9 °C for low filler addition and gradually narrows to almost 2 °C at the higher filler contents. Changes are similar for silica and titania. At the same time, we record changes in the shape of the glass transition thermogram. In particular, the glass transition shape seems to be double structured in the case of nanocomposites with 31 wt% silica and 11.5 wt% titania and higher. As filler content increases the secondary contribution at the high-temperature side gets more clear, while at the same time the height of the first contribution (low-temperature side) is increased, in terms of heat capacity change ΔC_p. This secondary contribution seems to be related to the strong polymer–filler interactions, on the basis of a polymer layer on the surface of the nanoparticles, completely or almost immobilized [41] or with highly reduced mobility. Similar observations have been made before in polymer nanocomposites, either in the form of changes in the shape of the response [26] or through significant changes of the heat capacity step at the glass transition [8,27,42–44]. This point will be further discussed later in this section and also in combination with TSDC and DRS results.

Having firm evaluation of the crystallization (specifically the fraction of crystallized polymer), we can calculate from the data for the glass transition, in particular from the heat capacity step, the amount of immobilized polymer X_{imm}, i.e. the amount of amorphous polymer which makes no contribution to the glass transition [41]. In terms of heat capacity change $\Delta C_{p,norm}$ as recorded from DSC and normalized with amorphous polymer fraction (Table 1) according to Eq. (3), we calculated X_{imm} using Eq. (4)

$$\Delta C_{p,norm} = \frac{\Delta C_{p,DSC}}{(1 - X_c)X_{PDMS}} \tag{3}$$

$$X_{imm} = 1 - \frac{\Delta C_{p,norm}}{\Delta C_{p,norm,PDMS}} \tag{4}$$

Despite any uncertainty in the ΔC_p values, X_{imm} was found to be almost constant between 0.73 and 0.83 (i.e. 73 and 83% of the non-crystallized polymer) in the nanocomposites for both silica and titania (Fig. 5). These results suggest that the amount of amorphous polymer which participates to the glass transition is also constant in the nanocomposites. It has been reported for semi-crystalline polymer nanocomposites that the presence of a certain constant amount of rigid amorphous phase (RAF) [45] around the individual lamellar crystals along with nanofillers which interact with the polymer lead to such results [46].

Following previous work [8], by applying a simplified model (inset of Fig. 5), which is mathematically described in the following equation [47]

$$d_{\text{int}} = \left[\left(v_{\text{int}}/v_{filler}\right)^{1/3} - 1\right] r_{filler} \tag{5}$$

where v_{int} and v_{filler} are the volume fractions of the interfacial (immobilized) polymer layer and fillers in the nanocomposites, respectively, while r_{filler} is the radius of the nanoparticles, d_{int} was calculated to be about 1–5 nm for PDMS/silica and about 20–40 nm for PDMS/titania (referred as d_{imm} in Table 1). The volume fraction calculations (vol%, Table 1) were made transforming weight fractions (wt%) and using standard values for the densities of silica, titania and PDMS (2.65, 4.23 and 1.62 g/cm^3, respectively). The decrease of d_{imm} with increasing filler content in Table 1 reflects simply overlapping of the interfacial layers of individual nanoparticles, which has not been taken into account in the simplified form of Eq. (5). The high difference between PDMS/silica and PDMS/titania d_{int} values is consistent with the results of characterization measurements (described above in Section 2.1) [23] about the interaction strength of titania particles with PDMS, which is higher in comparison with silica. With respect to absolute values for d_{imm}, such values come in agreement with previous work [8], as far as silica is concerned. High values of d_{int} have been also reported before in poly(methyl acrylate) (PMA)/clay nanocomposites [48]. Results on poly(methyl methacrylate) (PMMA)/silica nanocomposites [49] have shown that the length of polymer–filler interfacial effects are by tens of nanometers higher than the cooperativity length ξ of segmental motions [50]. Similar observations have been made for thin polystyrene films, where the size of cooperatively rearranging region is much smaller than the distance over which interfacial effects propagate [51]. We will come back to this point later in relation to DRS measurements.

3.2. TSDC measurements

The TSDC thermograms are presented in Fig. 6 for PDMS/silica and in Fig. 7 for PDMS/titania samples. In order to have better comparative evaluations, the depolarization current was normalized with the applied electric field, so that results for different samples can be compared to each other not only with respect to the

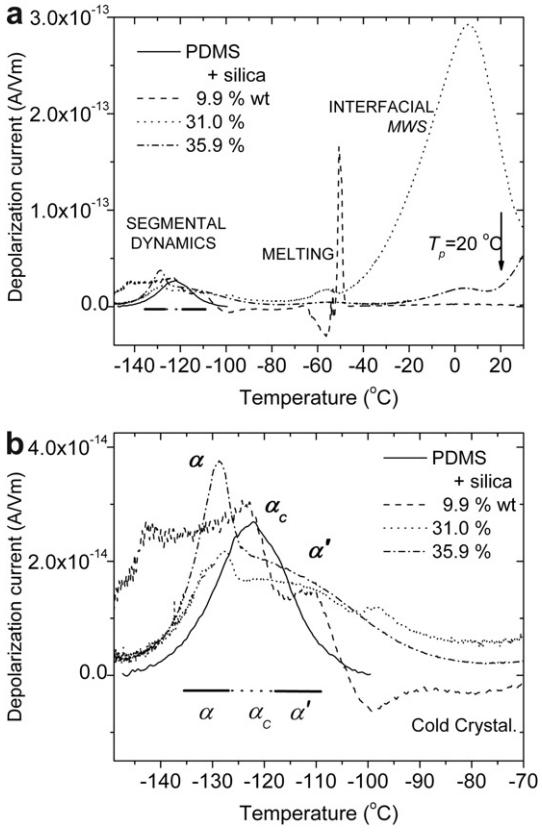

Fig. 6. Comparative TSDC thermograms for unfilled PDMS and PDMS/silica nanocomposites (a) overall behaviour and (b) in the region of glass transition.

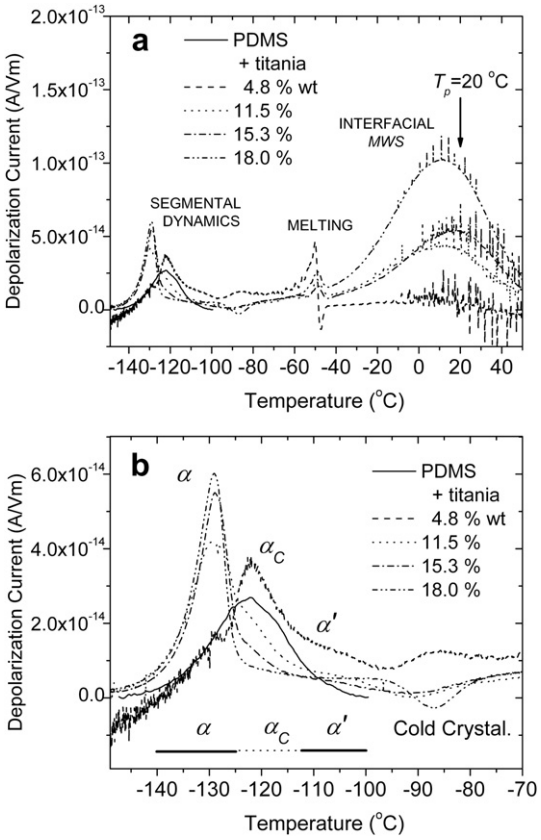

Fig. 7. Comparative TSDC thermograms for unfilled PDMS and PDMS/titania nanocomposites (a) overall behaviour and (b) in the region of glass transition. The reduction of the degree of crystallinity with filler content depresses the height of α_c relaxation and at the same time α, α' and MWS relaxations arise.

temperature position of a peak (time scale of the corresponding relaxation) but also with respect to the magnitude of a peak (dielectric strength of the corresponding relaxation). In the temperature range from −140 to −100 °C, i.e. in the range of the calorimetric glass transition (Fig. 1 and Table 1), complex spectra consisting of three peaks are well discerned, for both types of nanocomposites. We know that the equivalent frequencies of TSDC and DSC measurements [32] are in a similar range, so we suggest at this stage and will provide additional evidence for that later that the three peaks (relaxations), called α, α_c and α' in the order of increasing temperature, are dielectrically related with cooperative PDMS chain motions in the glass transition region.

It is interesting to discuss the systematic manner in which these three peaks contribute to the overall complex segmental dynamics in the nanocomposites (Figs. 6b and 7b). Being completely absent in unfilled PDMS, the magnitude of α' relaxation (between −120 and −95 °C) increases with filler content. The α_c relaxation (at about −123 °C) is faster and stronger than α' and its position is not affected directly by the nanoparticles. The strength of this relaxation decreases with decreasing degree of crystallinity X_c (Table 1). Simultaneously with the filler addition and depression of α_c the upcoming of α relaxation is observed at −130 to −128 °C. This statement will be confirmed later in DRS isothermal crystallization measurements.

The α' extends in a broader temperature region than α and α_c, which enhances our suggestions related to the observed changes in the shape of the glass transition in the DSC thermograms (insets to Fig. 1). Also, it seems that the broadened glass transition of unfilled PDMS recorded through DSC corresponds directly to α_c relaxation, while the sharp shaped glass transition, recorded for the highest silica and titania contents corresponds directly to α relaxation. At this point, the three relaxations can be clearly defined as: glass transition of free (bulk) polymer chains (α relaxation), reduced cooperative mobility of amorphous polymer confined between crystal regions (α_c relaxation) [43,52–54] and relaxation of the polymeric chains which are semi-bound on the nanoparticle surfaces (α' relaxation) [8]. Please note that α_c shows a similar strength for PDMS, PDMS/silica and PDMS/titania, while α relaxation is stronger in the case of titania and α' is stronger for silica. We can assume on the basis of the DSC results (very similar values of T_m for the two types of filler, Table 1) that the size and quality of the PDMS crystals are similar for both types of filler, giving similar position and dielectric strength to α_c relaxation. On the other hand, α and α' carry together the relaxation strength of the segmental dynamics of the amorphous polymer and, in this sense, it is reasonable that either of them increases at the expenses of the other. We will come back to this point in a more quantitative way later on the basis of DRS results.

The events recorded in the temperature range between −100 and −80 °C seem to be related to cold crystallization. The reason for recording cold crystallization by TSDC is the low heating rate in this technique (3 °C/min). Crystallization kinetics has been recorded before through anomalous behaviour in dielectric measurements in poly(ethylene oxide) (PEO) and poly(3-hydroxybutyrate) (PHB) [35].

The signal recorded between −65 and −40 °C corresponds to the melting of PDMS crystals. Electrical charges trapped inside or between crystals during cooling in the polarization step get massively disengaged while passing through the T_m region during heating and give rise to the response measured. In agreement with

this interpretation, the observed strength of the signal (respective current range in Fig. 7a for this melting process) increases with X_c.

The strong peak which follows at higher temperatures is due to the interfacial Maxwell–Wagner–Sillars (MWS) relaxation. MWS arises from the trapping and the subsequent release of charges at the interfaces between polymer and filler [8,55]. In the case of PDMS + 35.9 wt% a huge internal electric field opposite to the external applied field [56] was created during polarization. For that reason the main relaxation occurred as a negative (inverted) peak. So in Fig. 6 we present a respective measurement, in which the polarization temperature was −60 °C, so that MWS polarization was not activated. The strength of the interfacial MWS relaxation increases with filler content, almost linearly. In the case of PDMS/titania (Fig. 7a) small electric discharges are observed over the MWS curve. This is an indication of the highly branched particle structure or the too close distance between particles in general and comes in agreement with TEM results on the same materials [23].

By employing special techniques like Thermal Sampling [8], we gained supplementary evidence for the statements made above, in particular the assignment of the three relaxations in the glass transition region and evaluations about the activation energy and changes between α and α_c behaviour with temperature. Segmental dynamics, along with melting and MWS TSDC peaks, will be further followed in future work.

3.3. DRS measurements

DRS results will be comparatively presented here in the form of frequency (Fig. 8, isothermal plots) or temperature dependence of the imaginary part of dielectric permittivity (dielectric loss) ε'' (Fig. 9, isochronal plots). We focus here on segmental dynamics, i.e. on the dielectric relaxations α, α_c and α' corresponding to the TSDC response in the temperature range from −140 to −100 °C in Figs. 6 and 7.

Recorded at −110 °C, one can observe in Fig. 8 α_c and α relaxations of PDMS, PDMS + 31.0 wt% silica and PDMS + 15.3 wt% titania at around 1 and 50 kHz, respectively. Based on the values of the degree of crystallinity, as calculated from DSC measurements (Table 1), along with the strength and frequency range of the α_c relaxation for the two types of filler in PDMS, the identification of the two relaxations is similar to that in the TSDC results, compare Section 3.2. With the open symbols in Fig. 8 we follow the data of the isothermal measurements for the two nanocomposites at −75 °C. Significant changes are recorded here for α' relaxation, which is by far stronger and faster (by 2 orders of magnitude in frequency) in case of PDMS/silica, as compared to PDMS/titania, again in agreement with TSDC.

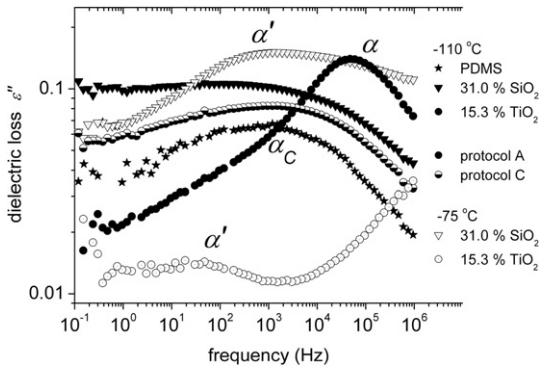

Fig. 8. Isothermal DRS plots of dielectric loss ε'' vs frequency for PDMS, PDMS + 31.0 wt% silica and PDMS + 15.3 wt% titania nanocomposites, at −110 °C (solid symbols) and −75 °C (open symbols).

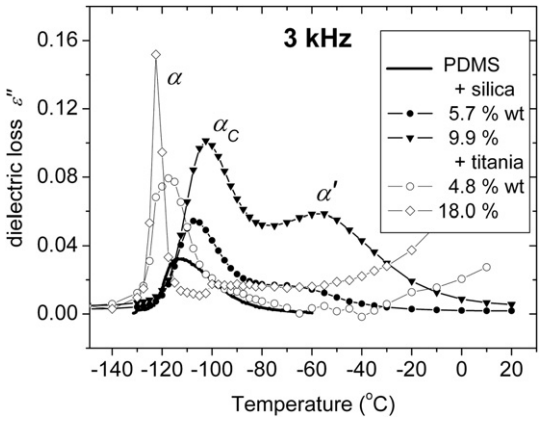

Fig. 9. Comparative isochronal plots of the imaginary part of dielectric permittivity ε'', replotted from DRS measurements at 3 kHz for PDMS/silica (solid symbols) and PDMS/titania nanocomposites (open symbols).

In the case of PDMS + 15.3 wt% titania at −110 °C, it is clear that the recorded relaxation is complex, as a superposition of α_c (~1 kHz) and α (~50 kHz) relaxations. The results described up to this point were obtained by measurements carried out under the thermal *protocol A* (almost amorphous polymer). Included in Fig. 8 are also data (semi-open circles) of measurements of the PDMS/titania sample under the *protocol C* (annealed at crystallization temperature, semi-crystalline polymer). For the polymer allowed to get crystallized, the segmental dynamics is mainly expressed as the broadened, weaker and slower α_c relaxation, which is reasonable on the basis of the DSC results.

Data recorded isothermally were replotted in Fig. 9 as isochronal $\varepsilon''(T)$ plots to facilitate direct comparison with the TSDC thermograms of Figs. 6 and 7. A higher frequency of 3 kHz was selected for the plots to suppress effects of conductivitry [33]. In general, α relaxation is stronger in the case of titania, and α_c and α' are stronger in the case of silica. The strength of α_c and α' shows significant variation with composition in PDMS/silica, but not in the case of PDMS/titania, while in both cases the temperature position of α_c and α' doesn't change significantly with composition. The results agree well with those of TSDC, while the slight shift to higher temperatures in Fig. 9, as compared to Figs. 6 and 7, arises from the higher frequency of presentation [8].

The isothermal $\varepsilon''(f)$ plots in Fig. 10 present spectra recorded every 15 min continuously for 3 h, to follow effects of crystallization at −105 °C. The temperature of −105 °C was selected on the basis of the DSC results in the crystallization region to enable following isothermal crystallization over a few hours. In the beginning we record segmental dynamics expressed exclusively as α relaxation. As time passes, the degree of crystallinity increases along with α_c relaxation. As α_c increases in magnitude, α is depressed and the spectra become complex, consisting clearly of two contributions (see bold lines in Fig. 10, at 90 and 135 min). Finally, after 3 h α relaxation is vanquished and α_c dominates the response of the sample. The weak increase of the ε'' response at the lower frequencies represents the incoming of α' relaxation into the measurement window. It would be interesting if we were able to record in a broader frequency range, at the same time, α' relaxation in the spectra of Fig. 10, expecting to verify that no significant changes would be observed during this isothermal experiment.

By plotting the frequency of maximum of ε'' against reciprocal temperature for the three segmental relaxations, the Arrhenius plot (activation diagram) of Fig. 11 was constructed. At this stage of presentation we prefer to rely only on the raw data, so no evaluation

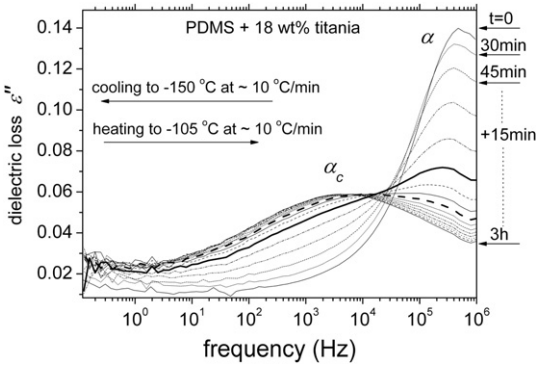

Fig. 10. Dielectric loss ε'' vs frequency for PDMS + 18 wt% titania nanocomposite, as recorded during isothermal crystallization at −105 °C. Segmental dynamics expression changes with time from α to α_C behaviour.

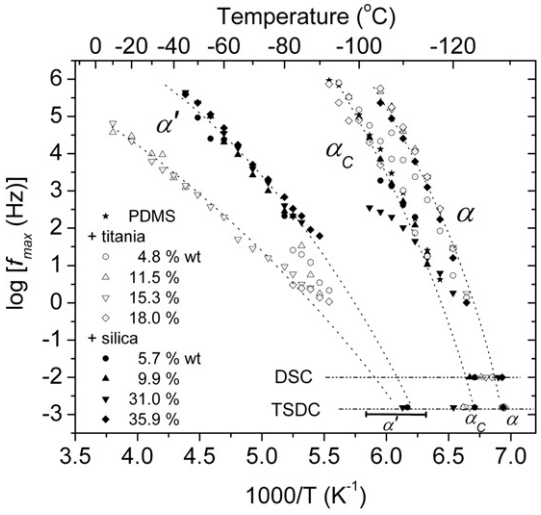

Fig. 11. Arrhenius plot of the segmental and interfacial dynamics for PDMS PDMS/silica and PDMS/titania nanocomposites. Respective points were added from TSDC and DSC techniques. Dotted lines (·····) were also added as guides for the eyes.

in terms of fitting of model functions to the experimental data was performed [8,33]. Included in the plot are also DSC and TSDC data at the equivalent frequencies of 10 [57] and 1.6 mHz [8]. The time scale of all relaxations for the various samples and thermal protocols can be discussed well using such plots. A main observation in Fig. 11 is that α and α_c have very similar frequency–temperature traces. The behaviour is typical for segmental dynamics, ruled by the Vogel–Tammann–Fulcher (VTF) behaviour [50] and practically not affected by the addition of nanoparticles. On the other hand, α' tends to be strongly separated from α and α_c, and its time scale is practically described by a straight line (Arrhenius behaviour [50]) characterized by lower activation energy (~0.52 and ~0.50 eV for silica and titania, respectively), as compared to α and α_c. The result is very similar to that observed for a different PDMS network filled with silica nanoparticles [8].

By taking a careful look on the Arrhenius plot (Fig. 11) in the region of α_c relaxation, we observe a departure of the respective points for PDMS + 31.0 wt% silica from the typical α_c behaviour. The departure is particularly strong at higher temperatures. Having in mind the DSC results for this sample (Table 1) we realize that as the temperature of the measurement increases, approaching to the calorimetric T_c, the degree of crystallinity is also increasing. Thus, a reasonable explanation for this departure from the typical α_c trend is that as temperature increases, the degree of crystallinity increases due to cold crystallization and the mobility of polymer chains gets continuously restricted (during the measurement) into the growing crystal regions. As a result, the segmental dynamics for this sample changes continuously from the behaviour of α at low temperatures to the behaviour of α_c at higher temperatures. At the highest temperatures of measurements for this sample the relaxation becomes even slower than the typical α_c trace (Fig. 11). This would suggest an effect of the method of crystallization (time–temperature profile) on segmental dynamics [34,53], which should be further followed in future work. This effect is not observed for the highest silica content (35.9 wt%), probably due to the low degree of crystallinity (Table 1): the segmental dynamics shows the behaviour of α at all temperatures of measurement (Fig. 11), although cold crystallization is observed in the DSC thermogram (Fig. 1a). Please note that in isothermal DRS measurements the sample stays at the temperature of measurement for several minutes, so cold crystallization can be particularly pronounced. A further comment with respect to Fig. 11 refers to the sample PDMS + 4.8 wt% titania. Probably due to the relative uncertainty in recording of the weak α' relaxation for this sample, the respective points seem to be shifted to lower temperatures from the typical trend for PDMS/titania measurements.

In the Arrhenius plot (Fig. 11) the α' relaxation traces look linear (Arrhenius behaviour), but judging from the respective TSDC temperature range we conclude that the best fitting to the data is given by the VTF equation

$$f = f_0 \exp\left(-\frac{DT_0}{T - T_0}\right) \tag{6}$$

where f_0 is a frequency constant, D is the fragility strength parameter and T_0 is the Vogel temperature [50,58]. After fixing the f_0 parameter to the phonon value 10^{13} Hz [33,58], by fitting Eq. (6) to our experimental data we obtained values for the D parameter. D is related to the steepness or fragility index m according to the following equation [59]

$$m = 16 + 590/D \tag{7}$$

The average fragility index values were calculated (Eq. (7)) to be 110, 97, 44 and 21 respectively for α, α_c, α' (of PDMS/silica) and α' (of PDMS/titania) relaxations. The uncertainty for these fragility values is about 5. Lorthior et al. have calculated similar values for α and α_c [52]. The VTF behaviour is indicative of cooperative relaxation mechanisms, so this is another strong indication that α' relaxation in these nanocomposites is indeed affiliated to segmental polymer chain motions (glass transition). The reduced fragility values of α', in comparison with α and α_c relaxations, is explained by means of reduced cooperativity of segmental motions [50]. Thus, our results suggest that the cooperativity length [60] is larger in the PDMS/silica than in the PDMS/titania nanocomposites.

Having now clear evidence about the origins of the relaxations described above and in combination with DSC and DRS results, we can calculate the reduced mobility polymer fraction X_{int} (the fraction of polymer in the interfacial layer, Fig. 12) by the following equation

$$X_{\text{int}} = \frac{\Delta\varepsilon_{\alpha'}(1 - X_c)}{\Delta\varepsilon_{\alpha'} + \Delta\varepsilon_{\alpha+a_c}} \tag{8}$$

where $\Delta\varepsilon$ is the dielectric strength of each relaxation [33] and X_c is the degree of crystallinity for each sample (Table 1). The surface area under the loss peak was taken as a measure of the dielectric strength of the corresponding relaxation. The results show that in the case of PDMS/silica the interfacial polymer fraction increases from 0.05 to 0.55 at the highest filler content (Fig. 12), while at the same time the degree of crystallinity drops from 0.42 to almost

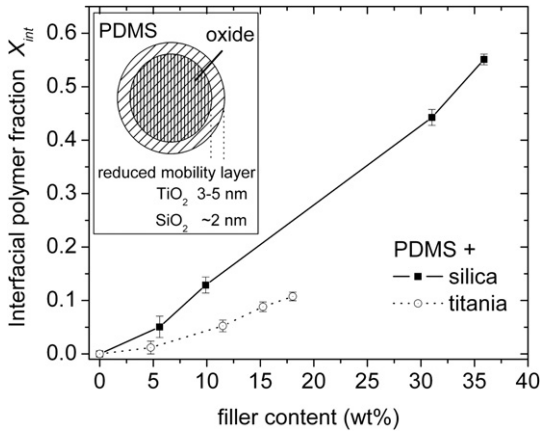

Fig. 12. The fraction of PDMS with reduced mobility vs silica and titania content obtained from Eq. (5). The inset shows the simplified model used to calculate the thickness of the interfacial layer.

0 (Table 1). In the case of PDMS/titania X_{int} is significantly lower and increases from 0 to 0.14 at the highest loading (Fig. 12), while X_c drops from 0.43 to 0.13 (Table 1). Following the same procedure as with the respective DSC results, by exploiting the information from the TEM measurements on the morphology and the dimensions of the nanoparticles [23], it is possible to make an estimation of the thickness of the interfacial layer d_{int}, now from the DRS results. By applying Eq. (5), d_{int} was calculated to be ~2 nm for PDMS/silica and 3–5 nm for PDMS/titania nanocomposites (Fig. 12). Combining our conclusions for the changes in segmental dynamics with the X_{int} trends (Fig. 12), we get additional support for the large total interactive surface area of the smaller silica particles and the respective smaller total interactive surface area of the larger titania particles.

Although these results about the estimation of the interfacial influence (d_{int}) of the fillers on the PDMS chain mobility agree with the respective DSC values (d_{int}), in the sense that the restriction is higher in the case of titania, the absolute values are different for the two techniques, larger in the case of DSC, especially for the titania nanocomposites. We should keep in mind that in DRS measurements X_{int} was estimated through the direct and additive contribution of the nanoparticles to the segmental dynamics (α' relaxation), whereas in DSC measurements X_{imm} was estimated more indirectly through the missing of the corresponding contribution to the heat capacity jump at the glass transition (reduction of ΔC_p step). Moreover, the DRS measurements provide, through the variation of both independent variables, frequency and temperature, the possibility to follow the evolution of the isothermal $\varepsilon''(f)$ spectra (and, thus, the evolution of X_{int}) with temperature [26]. On the other hand, we observe in Figs. 7 and 9 that as X_c increases the whole dielectric response in the glass transition region gets lower. It is not clear at this stage to which extent the reduction of the fraction of the amorphous polymer and the constraints imposed by the polymer crystallites (i.e. the amount and influence of the rigid amorphous phase [45]), on the one hand, and a direct effect of the nanoparticles through the reduction of molecular mobility in the interfacial layer, on the other hand, are responsible for that [61]. Further DRS experiments and analysis of the data by fitting model functions are in progress to quantitatively further follow this point. Please also note that by using Eq. (8) to calculate X_{int} it is implicitly assumed that the dielectric permittivity of PDMS is the same in the interfacial layer and the bulk amorphous and crystalline fractions. It is interesting to note in this connection that DSC, DRS and TSDC measurements in (amorphous) polyurethane/clay nanocomposites show, in agreement to each other, that a fraction of polymer is immobilized, making no contribution to the measured response by neither of the three techniques, and that this fraction is larger by DRS than by DSC [42].

4. Conclusions

The effects of nanoparticles on glass transition and molecular dynamics were studied in two series of PDMS/silica and PDMS/titania nanocomposites by employing calorimerty and dielectric techniques. Extended measurements using different thermal treatments showed that the good dispersion and strong interactions of the nanoparticles with PDMS restrict crystallization and segmental mobility of the polymer. In addition to calorimetry, the dielectric DRS and TSDC techniques provided significant information on the overall mobility, mostly on the segmental dynamics of the polymer (dynamic glass transition), which was found to consist of three discrete and well defined relaxations. These relaxations arise from the bulk (unaffected) polymer (α relaxation), the mobility of polymer chains restricted between condensed crystalline regions (α_c relaxation) and the segmental dynamics in an interfacial polymer layer around (or, in general, close to) the nanoparticles (α' relaxation).

Compared with PDMS/silica in this work and in a previous work with a slightly different PDMS [8], the effects were stronger in the series of PDMS/titania nanocomposites. These are characterized by stronger polymer–filler interactions, reflected in a shift of α' to lower frequencies/higher temperatures and a larger thickness of the interfacial layer.

At temperatures lower than the melting point of the crystalline PDMS phase, the neat polymer (zero filler content) is presented in two phases: as crystallized (immobilized) and amorphous within the crystals (lamellar or/and RAF/low mobility). As filler content increases, some amount of PDMS becomes bound (reduced mobility) on the surfaces of the particles due to hydrogen bonding and the other two phases described above get restricted, while amorphous islands of PDMS (bulk/free mobility) start growing between the crystals and the nanoparticles (four phases). At the higher loadings the crystallization is practically absent along with the lamellar/RAF and the polymer is mainly composed of bulk and bound on the nanoparticles (two phases). For both types of filler the amount of PDMS which shows amorphous properties, participating in the glass transition, seems to be constant at ~12 wt% of the nanocomposite. This molecular view, which emerges from the experimental results, indicates some kind of self-organization of the systems under investigation, where the polymer is composed of different phases and the composition changes in a continuous way under the external influences of the addition of nanoparticles and the variation of the temperature.

It should be noted, from the methodological point of view, that, although the three techniques employed agree with each other in the overall picture of reduction of molecular mobility in the nanocomposites, there are distinct differences between the quantitative results obtained by DSC, on the one hand, and by the two dielectric techniques, on the other hand. This point should be further followed in future work.

With respect to the dielectric techniques, results and conclusions in the present paper are based mainly on the raw data and the overall spectra. Thermal sampling TSDC measurements in future work may provide more quantitative information on a possible distribution of relaxation times and glass transition temperatures in the interfacial layer [8,51]. Also analysis of the DRS data in the glass transition region by fitting model functions, which is in progress, may provide among other information on the temperature dependence of the thickness of the interfacial layer [8]. Finally,

DSC measurements with temperature modulation (TMDSC) may provide further information on polymer mobility near the polymer crystals and the nanoparticles [46,62].

Acknowledgements

The research leading to these results has received partial support from the European Community's Seventh Framework Programme [FP7/2007-2013] under grant agreement no. 218331 NaPolyNet.

References

[1] Sperling LH. Introduction to physical polymer science. New Jersey: Wiley; 2006.
[2] Mark J. Polym Eng Sci 1996;36:2905–20.
[3] Bokobza L, Chauvin JP. Polymer 2005;46:4144–51.
[4] Coleman JN, Cadek M, Ryan KP, Fonseca A, Nagy JB, Blau WJ, et al. Polymer 2006;47:8556–61.
[5] Papakonstantopoulos GJ, Yoshimoto K, Doxastakis M, Nealey PF, de Pablo J. J Phys Rev E 2005;72:031801.
[6] Rodriguez Hernandez JC, Monleon Pradas M, Gomez Ribelles JL. J Non-Cryst Solids 2008;354:1900–8.
[7] Hongbin L, Steven N. Macromolecules 2003;36:4010–6.
[8] Fragiadakis D, Pissis P. J Non-Cryst Solids 2007;353:4344–52.
[9] Bilotti E, Fischer HR, Peijs T. Appl Polym Sci 2008;107:1116–23.
[10] Ramanathan T, Abdala AA, Stankovich S, Dikin DA, Herrera-Alonso M, Piner RD, et al. Nat Nanotech 2008;3:327–31.
[11] Paul DR, Robenson LM. Polymer 2008;49:3187–204.
[12] Rittigstein P, Torkelson JM. J Polym Sci Part B Polym Phys 2006;44:2935–43.
[13] Logakis E, Pandis C, Peoglos V, Pissis P, Stergiou C, Pionteck J, et al. J Polym Sci Part B Polym Phys 2009;47:764–74.
[14] Lincoln DM, Vaia RA, Wang ZG, Hsiao BS. Polymer 2001;42:1621–31.
[15] Tsagaropoulos G, Eisenberg A. Macromolecules 1995;28:6067–77.
[16] Kirst K, Kremer F, Litvinov V. Macromolecules 1993;26:975–80.
[17] Litvinov V, Spiess H. Macromol Chem Phys 1991;192:3005–19.
[18] Arrighi V, McEwen I, Qian H, Prieto M. Polymer 2003;44:6259–66.
[19] Matejka L, Dukh O, Kolarik J. Polymer 2000;41:1449–59.
[20] Arrighi V, Higgins J, Burgess A, Floudas G. Polymer 1998;39:6369–76.
[21] Berriot J, Montes H, Lequeux F, Long D, Sotta P. Macromolecules 2002;35:9756–62.
[22] Robertson CG, Lin CJ, Rackaitis M, Roland CM. Macromolecules 2008;41:2727–31.
[23] Bokobza L, Diop AL. Express Polym Lett 2010;4:355–63.
[24] Vralstad H, Spets Ø, Lesaint C, Lundgaard L, Sjoblom J. Energy Fuels 2009;23:5596–602.
[25] Syunyaev RZ, Balabin RM. J Dispers Sci Technol 2007;28:419–24.
[26] Fragiadakis D, Pissis P, Bokobza L. Polymer 2005;46:6001–8.
[27] Sargsyan A, Tonoyan A, Davtyan S, Schick C. Eur Polym J 2007;43:3113–27.
[28] Miwa Y, Sugino Y, Yamamoto K, Tanabe T, Sakaguchi M, Sakai M, et al. Macromolecules 2004;37:6061–8.
[29] Gedde UW. Polymer physics. London: Chapman & Hall; 1995.
[30] Dewimille L, Bresson B, Bokobza L. Polymer 2005;46:4135–43.
[31] Sorai M, editor. Comprehensive handbook of calorimetry and thermal analysis. West Sussex: Wiley; 2004.
[32] Brauenlich P. Thermally stimulated relaxation in solids. Berlin: Springer; 1979.
[33] Kremer F, Schoenhals A, editors. Broadband dielectric spectroscopy. Berlin: Springer; 2002.
[34] Wurm A, Soliman R, Schick C. Polymer 2003;44:7467–76.
[35] Napolitano S, Wübbenhorst W. Macromolecules 2006;39:5967–70.
[36] Aranguren M. Polymer 1998;39:4897–903.
[37] Clarson SJ, Dodgson K, Semlyen JA. Polymer 1985;26:930–4.
[38] Soutzidou M, Panas A, Viras K. J Polym Sci B 1998;36:2805–10.
[39] Carlberg M, Colombini D, Maurer FH. J Appl Polym Sci 2004;94:2240–9.
[40] Sundararajan PR. Polymer 2002;43:1691–3.
[41] Bershtein VA, Egorova LM, Yakushev PN, Pissis P, Sysel P, Brozova L. J Polym Sci Part B Polym Phys 2002;40:1056–69.
[42] Kripotou S, Pissis P, Savelyev YV, Robota LP, Travinskaya TV. J Macrom Sci Part B Phys 2010;49:86–110.
[43] Raftopoulos KN, Pandis Ch, Apekis L, Pissis P, Janowski B, Pielichowski K, et al. Polymer 2010;51:709–18.
[44] Klonos P, Pissis P, Gun'ko VM, Kyritsis A, Guzenko NV, Pakhlov EM, et al. Colloids Surf A 2010;360:220–31.
[45] Dobbertin J, Hensel A, Schick C. J Thermal Anal Calorimet 1996;47:1027–40.
[46] Wurm A, Ismail M, Kretzschmar B, Pospiech D, Schick C. Macromolecules 2010;43:1480–7.
[47] Pelster R, Simon U. Colloid Polym Sci 1999;277:2–14.
[48] Miwa Y, Drews AR, Schlick S. Macromolecules 2006;39:3304–31.
[49] Priestley RD, Rittigstein P, Broadbelt LJ, Fukao K, Torkelson JM. J Phys Condens Matter 2007;19:205120.
[50] Donth E, editor. The glass transition: relaxation dynamics in liquids and disordered materials. Springer series in materials science, vol. 48. Berlin: Springer; 2001.
[51] Ellison CJ, Torkelson JM. Nat Mater 2003;2:695–700.
[52] Lorthioir C, Alegria A, Colmenero J, Deloche B. Macromolecules 2004;37:7808–17.
[53] Napolitano S, Wübbenhorst W. J Non-Cryst Solids 2007;353:4357–61.
[54] Yu L, Cebe P. J Polym Sci Part B Polym Phys 2009;47:2520–32.
[55] Hedvig P. Dielectric spectroscopy of polymers. Bristol: Adam Hilger; 1977.
[56] Page KA, Adachi K. Polymer 2006;47:6406–13.
[57] Vatalis AS, Kanapitsas A, Delides CG, Pissis P. Thermochim Acta 2001;372:33–8.
[58] Richert R, Angell CA. J Chem Phys 1998;108(21):9016–26.
[59] Boehmer R, Ngai K, Angell CA, Plazek DJ. J Chem Phys 1993;99:4201–9.
[60] Sappelt D, Jackle J. J Phys A Math Gen 1993;26:7325–41.
[61] Huo P, Cebe P. Macromolecules 1992;25:902–9.
[62] Xu H, Cebe P. Macromolecules 2004;37:2797–806.